

The emergence of the two cell fates and their associated switching for a negative auto-regulating gene

Zhenlong Jiang^{ac} (equal contribution), Li Tian^a (equal contribution), Xiaona Fang^a (equal contribution), Kun Zhang^a (equal contribution), Qiong Liu^a (equal contribution), Qingzhe Dong^a, Erkang Wang¹, Jin Wang^{abc*}

^aState Key Laboratory of Electroanalytical Chemistry, Changchun Institute of Applied Chemistry, Chinese Academy of Sciences, Changchun, Jilin, 130022, China

^bDepartment of Chemistry, Physics and Applied Mathematics, State University of New York at Stony Brook, Stony Brook, New York, 11794-3400, USA

^cCollege of Physics, Jilin University, Changchun, Jilin, 130012, China

* Corresponding author. Tel: +1-631-816-5920, Fax: +1-631-632-7960.

E-mail address: jin.wang.1@stonybrook.edu

July 5, 2017

Abstract

Decisions in the cell that lead to its ultimate fate are important for cellular functions such as proliferation, growth, differentiation, development and death. Understanding this decision process is imperative for advancements in the treatment of diseases such as cancer. It is clear that underlying gene regulatory networks and surrounding environments of the cells are crucial for function. The self-repressor is a very abundant gene regulatory motif, and is often believed to have only one cell fate. In this study, we elucidate the effects of microenvironments mimicking the epigenetic effects on cell fates through the introduction of inducers capable of binding to a self-repressing gene product (protein), thus regulating the associated gene. This alters the

effective regulatory binding speed of the self-repressor regulatory protein to its destination DNA without changing the gene itself. The steady state observations and real time monitoring of the self-repressor expression dynamics reveal the emergence of the two cell fates, The simulations are consistent with the experimental findings. We provide physical and quantitative explanations for the origin of the two phenotypic cell fates. We find that two cell fates, rather than a single fate, and their associated switching dynamics emerge from a change in effective gene regulation strengths. The switching time scale is quantified. Our results reveal a new mechanism for the emergence of multiple cell fates. This provides an origin for the heterogeneity often observed among cell states, while illustrating the influence of microenvironments on cell fates and their decision-making processes without genetic changes.

Keywords: gene expression | self-repressor | bimodality | cell fate decision making

Significance

It is often believed that genotypes determine phenotypes. Many studies have focused on genetic mutations rather than environmental changes or epigenetics. Here, we design a simple self-repressing gene circuit in *Escherichia coli*. We elucidate the effects of microenvironments or epigenetics on gene expressions through the introduction of inducers capable of binding to the self-repressor regulatory protein. This slows down the effective binding (regulation strength) of the regulatory protein to DNA. Despite the long-held belief that only one cell fate is present for the self-repressor, we observe that at some induction conditions, cells show two expression states, indicating two cell fates. Real-time monitoring of self-repressor expression during cell growth reveals the switching dynamics for cell fate decision-making between these two populations.

Introduction

Uncovering the origin of the phenotypes or fates of the cell and their associated switching is important for the full understanding of cell functions such as proliferation, growth, differentiation, development, and death. This remains

a challenging issue in biology. It is clear that the underlying gene regulatory networks are crucial in determining the function of the cell (1-6), and it is often believed that the genotype determines the phenotype (7-11). Recently, some studies have indicated that microenvironments or epigenetics can also alter the fates of the cell or its phenotypes even with the same genotypes (12-18). In other words, there is a possibility that apart from mutating the genes or the nodes themselves in the gene circuit, changing the underlying gene regulatory wirings among the genes or nodes in the regulatory network can alter the cell phenotypes or fates. In this study, we aim to study how altering gene regulation determines cell fates.

Negative auto-regulation is abundant: it is found in nearly 50% of the feedback loops in gene regulatory networks. It is widely believed that negative auto-regulation leads to a reduction of the gene expression noise, an increase of gene response times, an induction of possible oscillatory gene expression, and an improvement of the stability of proteins produced by the underlying gene networks (19-26). Despite these novel findings, most experimental studies have been focused on the influences of the genetic structures themselves, rather than the environmental or the epigenetic effects on the self-repressor.

For a self-repressing system, the expression distribution is commonly more concentrated and well-distributed (27). Many previous investigations have reached similar conclusions, observing only one cell fate (25, 28-30). However, these experiments were performed mostly in simple organisms such as bacteria, for which it is often assumed that the speed of regulatory protein binding to the corresponding DNA for switching is significantly faster than the synthesis and degradation of the corresponding regulatory proteins. In fact, in most organisms, cell complexes such as the nuclei inside mammalian cells may give rise to effectively slower processes of the underlying gene regulatory binding, due to environmental complexities such as epigenetic effects through histone modification or DNA methylation. That is, the effective rates of binding/unbinding of the regulatory proteins to the DNA can be comparable to, or even slower than, the production and degradation rate of the regulatory proteins (31). Modeling studies (32, 33) indicate that, in this case, the protein expressions of a negative feedback loop may not always show a simple single steady state, but instead can show two steady states, resulting in two different cell fates. Since the auto-regulation circuit involves only a single gene, it is the simplest gene regulation in *in vivo*. We will show experimentally that this simple gene auto-regulation circuit can lead to dif-

ferent cell fates or phenotypes under specific conditions, rather than that of only one cell fate as is commonly expected.

Results

Self-Repressing Gene Circuit and Non-Regulatory Gene Circuit

In this study, we have designed and constructed a purely negative auto-regulation feedback loop circuit (self-repressing gene circuit) in *Escherichia coli* (*E. coli*). The Ptet promoter including two *tetO* operons controls the production of its repressor, *TetR*. Meanwhile, the *TetR* was fused with a fluorescence protein (Venus) for experimental measurements of the *TetR* expressions. The inducer, aTc (anhydrotetracycline), was introduced to mimic environmental influences on expressions of the self-repression system. In the presence of an inducer, the repressor *TetR* can change its conformation and dissociate from specific binding sequences of the DNA (*TetO*). This allows for the transcription of *TetR*-Venus (Figure 1A). In order to avoid fluctuations in copy numbers of the plasmids, the constructed circuit in the plasmid was integrated into the chromosome of *E. coli*. We also constructed a series of self-repressing circuits with different affinities to the *TetR* protein (MG::PR-WT, MG::PR-1G) (Figure S2). We chose MG::PR-8T as the main circuit of this study for its stability and bimodal behavior. To compare this with our self-repressing circuit construction MG::PR-8T, we designed a non-regulatory circuit as a control group: the MG::PR-8T-P39K circuit (Fig. 1B).

The Expression Distributions of the Self-Repressor Gene Circuit under Microscopy

To obtain the expressions of *TetR* under different induction conditions, we measured the average fluorescence signals of the reporter protein Venus for the strain of MG::PR-8T at different inducer concentrations (300 ng/mL-1500 ng/mL) across cell populations using a wide-field fluorescence microscope. Cells were collected and measured after being cultured in M9 medium and induced by aTc for 4~6 hours to a logarithmic phase. To ensure accuracy of the expression distribution, we collected no less than 10^3 cells to measure

for each sample. All expression distributions under different induction concentrations are shown in Figure 2. The results indicate that *TetR* expression distributions vary with inducer (aTc) concentrations. Under low inducer concentrations, the expression levels of the negative regulated gene circuit were quite low, and this gene can be considered to be in the “off” state for a long time. With increased inducer concentrations, the expression levels were significantly enhanced (Fig. 2A). From the results shown in the microscope, we can clearly see that when inducers are added to the system, the repressor *TetR* can no longer prevent the transcription of *TetR*. When the inducer concentrations are high enough (such as 1400ng/mL and 1500ng/mL), the steady state expression distribution can become bimodal, with two states of low and high expression levels. Meanwhile, the percentage of the cells in the low expression state gradually increases with the increase of the inducer concentrations (Fig. 2A). Under high inducer concentrations, the coexistence of both phenotypes characterized by the bimodal steady state distributions of the fluorescence intensities can be clearly seen (Fig. 2E). When we further compare the images in Fig. 2D and 2E, it is clear to see that one section of the cells in Fig. 2E is brighter, while other sections were dimmer, compared to most of the cells in Fig. 2D. As can be seen from the microscopy images, the morphologies of the bacteria cells are not influenced by the aTc inducers at a concentration level of 1500 ng/mL (Fig. 2E). The corresponding distributions of those images are given in Fig.2A. In our control experiments, similar behaviors are not found in the MG::PR-8T-P39K non-self-repressing gene circuit under the same conditions (Figure S7). This indicates that the two expression states of *TetR* were due to the self-repressing circuit, rather than other factors such as the influences of the inducers on the cells.

Fano Factor and Inhibition Curve

To further understand our experimental observations, we need to quantify the degrees of fluctuations. This can be measured by the Fano factor quantified as the variance of the observable divided by the mean value (34). The Fano factor is equal to one ($F = 1$) if the distribution of the observable is exactly Poisson. A large Fano factor implies significant statistical fluctuations deviating from Poisson (Figure 3A). Qualitatively, the Poisson distribution should be a good approximation for the individual “on” and “off” states when the observed distribution of fluorescence intensity is bimodal, because each gene state can produce proteins almost independently of gene switching.

However, the overall Fano factor for the combined probability distribution of “on” and “off” states is much larger than 1. This is because the system is close to a two peak (Non-Poisson) distribution with different means summed together, producing large statistical fluctuations deviating from the single Poisson distribution. This indicates that two Poisson processes added together will not lead to a Poisson distribution. The analysis of the coefficient of variation (CV) in Figure S6 also illustrates this same conclusion.

Furthermore, we investigated the inhibition curve, which describes the proportion of the bacteria with a fluorescence intensity lower than a certain value (Figure 3B). We can see that the proportion of the gene in its inhibited state first decreases at low concentrations of inducer (up to aTc concentration at 1200 ng/mL) and then increases as the inducer concentration becomes higher. More inducers introduce more interactions with the *TetR* molecules. This slows down the effective binding of the *TetR* to the DNA. Therefore, the gene has more times to be in its “on” state and less of a chance of being at the inhibition state (less inhibition capability from aTc 300 ng/mL to 1200 ng/mL). More *TetR* proteins will be synthesized as a result. At certain concentrations of inducer aTc (1200 ng/mL), the number of free *TetR* molecules synthesized from the gene’s “on” state increases, resulting in a comparable number of *TetR* molecules to aTc molecules. This will lead to more effective regulatory binding of *TetR* to DNA. Finally, there are more chances of the gene being in its “off” state. We suggest that the increasing number of the proteins produced as a result of the presence of more inducers at this concentration range of aTc (1200-1500 ng/mL) will eventually promote the probability of inhibition for gene switches, since more regulatory proteins are synthesized and available for inhibition when the inducer concentration becomes higher. At this condition, although the total protein expression is higher with the increase of inducer concentration, it is not high enough that the proportion of the bacteria in the inhibited state increases due to self-repressing regulation, leading to stronger effective inhibition. At extremely high aTc concentrations (beyond 1900 ng/mL), one expects that the number of the available regulatory molecules becomes far beyond the one needed for inhibition and high expression peak should dominate. However, the aTc the toxicity from aTc as antibacterial agent to the cells becomes effective. It is therefore not feasible to observe the healthy cell expression distribution at this extremely high concentration of aTc.

The Dynamics of *TetR* Expression in Real Time

We have seen that the self-repressing circuit can give a bimodal distribution. In order to further explore the underlying mechanism of this behavior, we monitored the dynamics of *TetR* expression in real time. We tracked cells during their growth and division on a microscope with a FCS2 (Focht Chamber System 2, Bioptechs) system which provides aTc continuously to guarantee the cells growing in the right environments (continuous flow of adequate nutrients from fresh medium (M9) through the cells on agarose pad) and avoids potential issue of heterogeneity of the environments. As shown in Fig. 4B, upon aTc induction, two types of cell responses were observed: the fluorescence intensity either changed significantly or almost remained the same. When we track cells in real time, we can see that, some cells switch between bright and dim, while other cells stay with similar brightness (Fig. 4B). The resulting fluorescence distribution is thus bimodal and a fluorescence threshold can be defined for each cell in its most probable induction state. The use of a microfluidic device, coupled with cell tracking and fluorescence measurements, allows us to generate fluorescence trajectories for a single cell on reasonable time scales (~ 300 minutes) for a single trajectory. Based on this, we collected 28 micro-colony movies and chose 163 fluorescence trajectories. We observed that the trajectories of a single cell fluorescence fluctuated significantly. We collected about 8200 fluorescence intensity data points corresponding to the selected trajectories. Several representative trajectories with significant fluctuations were shown to demonstrate the existence of two states (From Figure 4A-B, Figure S8, Movie S1 and Movie S2).

Two Cell State Identifications by Hidden Markov Chain Modeling

In order to explore the underlying mechanism of the bimodality, we collected the statistics of the fluorescence intensity obtained from the trajectories. The distribution of these intensities exhibits two peaks, suggesting that most of the initial cells are either in a high expression state or in a low expression state in their progeny. We then used a Hidden Markov Chain Model (HMM) (35) to fit the real time trajectories and identify the cell states, and then simulate the distribution of the fluorescence intensity (Figure 4C). To assign protein expression states and the rates of inter-conversion between them, we

performed data fitting using the HMM. From the HMM analysis, we obtained a correlation coefficient of 0.975 between the measured and simulated trajectories after identifying the cell states and quantifying their switching rates. The simulated distribution fits with the measured distribution well. From the HMM analysis, we further determined the center positions of the peaks to be at 2.690 and at 2.933 in logarithm of fluorescence intensity. The variances of the individual peak distributions are at 0.085 and at 0.080, respectively. For our system, the probability in the high expression state is around 0.401, and we can also see that the probability in the low expression state is around 0.599.

In the high expression state, the system will continue its behavior with a probability of 0.963 (the switching or residence time will be discussed in the next section). There is a small chance, with the probability of 0.037, to switch to the low expression state from the high expression state. Meanwhile, there is additionally a probability of 0.023 that the system will switch to the high expression state from the low expression state, instead of remaining in the low expression state.

The Average Residence Times of the Protein Expression States

To estimate the average residence times of the protein expression state, we distinguished the states from the trajectories using HMM analysis and calculated the residence times of each state (Figure S11). For each trajectory, we counted the total residence times and the number of the state changes. The average residence times were calculated as the quotient of the total residence times and the number of states changed.

The length of the test fluorescence trajectory is finite and limited. This may lead to some errors in estimating the transition times. We take this into account in determining the time scale of the transitions. The average residence time of the high expression state is estimated to be about 92~103 minutes, and that of the low expression state is estimated to be about 151~182 minutes. The average residence time can be used to quantify the switching time between two cell fates. Therefore, the switching time from high (low) expression to low (high) expression can be estimated to be about 92~103 (151~182) minutes. Through fluctuations, the bimodal distribution can be maintained in a dynamic balance between the high expression “on” state

and the low expression “off” state. When the inducer concentration is fixed, the increasing number of proteins will promote the inhibition probability of gene switching. Therefore, the cells in the high expression state will have a tendency to migrate to the low expression state. Conversely, the cells with low expressions will be more likely to move towards the “on” state. Therefore, the cells in the low expression state will also have a tendency to migrate to the high expression state.

Physical Origin of the Two Cell Fates

Intuitively, from a molecular perspective, we know that the transcription process is suppressed when the promoter site of the DNA is occupied by a repressor (the gene is “off”), and enhanced when the repressor is dissociated from DNA (the gene is “on”). When the inducer concentration is low, increasing the inducer concentration will increase the binding of aTc to *TetR* and slow down the effective binding of *TetR* to the promoter. This lessens the chance of the genes being in an “off state” and conversely increases the possibilities of the gene being at the “on state”, resulting in higher expressions. This explains the shift of the expression peak from low to high as inducer concentration increases. When the inducer concentration further increases to sufficiently high values, the chance of having free *TetR* molecules will be higher (comparable number of *TetR* molecules to that of aTc molecules) as a result of synthesis. More *TetR* molecules will have increased chances of binding to the promoter site and will therefore display more repressive activity. This will lead to the emergence of the low expression peak and therefore bimodal distribution of the copy number in mRNA and proteins. Further increases of the inducer concentrations will lead to more free *TetR* molecules, with a resulting greater weighting of low, rather than high, expression peaks. This explains the trend of expression peaks as seen in Fig. 2A.

When the effective binding/unbinding is much faster compared to the synthesis/degradation, the gene state changes rapidly. The interactions and the mixings become stronger between the two gene states, and therefore also between the two corresponding protein concentration peaks. For the self-repressor, decreasing the effective binding (increasing the inducer concentrations in our study) promotes the generation of more proteins which in turn shows greater repressive activity. This leads to the high concentration peak moving towards a lower concentration. On the other hand, increasing the binding (decreasing the inducer concentrations in our study) represses the

generation of the proteins, and so fewer proteins produced bind effectively to DNA. This in turn promotes production of *TetR* molecules. It leads to the low concentration peak moving outward towards a higher concentration. As a result, the two peaks from the non-adiabatic limit (e.g. high aTc concentrations at 1400 ng/mL, slower binding) meet in the adiabatic limit (e.g. lower aTc concentration at 1300 ng/mL, faster binding) of the fast binding and merge into a single peak.

Gene switching is often rapid in bacterial cells. However, slow gene switching controlled by regulatory proteins binding/unbinding to the promoters can also be significant for gene expression dynamics. In eukaryotic cells and some prokaryotic cells, binding/unbinding may be comparable to or even slower than the corresponding synthesis and degradation due to epigenetic effects or complex microenvironments. By studying how the introduction of the inducers effectively weakens gene regulation in bacteria, we mimicked gene regulation dynamics in more complex eukaryotic cells. Through increasing inducer concentrations, we achieved effectively slower regulatory binding relative to synthesis and degradation. In other words, the introduction of the inducers in the bacteria leads to an additional time scale for regulatory binding. This mimicked the additional time scales for regulatory binding from including the histone modifications and DNA methylations in eukaryotic cells. This slower regulatory binding to inducers will lead to prolonged times of genes being in the “on state” in addition to the time spent in the “off state”, originated from the fast binding without inducers. As a result, both “on” and “off” states of genes may emerge. This is the physical mechanism of bimodality. In other words, the fast regulatory binding mimicked stronger interactions while the slow regulatory binding mimicked the weaker interactions among genes. While stronger interactions give more constraints to the system and therefore fewer degrees of freedom for the expressions (single peak expression), the weaker interactions will constrain the system less and therefore result in more degrees of freedom for the expressions (e.g., double peak expressions). Through the steady state and the real time observations of the dynamics of the self-repressor in the experiments, we observed the robust emergence of the bimodal gene expression distribution for the self-repressor.

Stochastic Simulations of Bimodality

We further explored the stochastic dynamics of self-regulative feedback genes through a mathematical model, which can be used to explain and simulate

the experimental observations (Figure 3C). The mathematical model clarifies the underlying mechanism of how bimodality emerges. Under faster regulation binding, the self-repressor is forced to stay in the repressed state. This is because once produced, the regulatory protein immediately binds to the gene and therefore represses protein production. In our study, slower binding of the regulatory protein to the gene is realized through the inducer binding to the regulatory protein, which effectively blocks the ability of the protein to bind to the promoter. Under slower regulatory binding, the self-repressor may function in two different ways: it may bind to the DNA for some time and repress protein production, or unbind from the DNA for some time, leading to increased protein production. This generates two cell phenotypes. Furthermore, due to the intrinsic statistical fluctuations of the number of proteins, there is a possibility of switching between the high expression and low expression state. We have observed such phenotypic switching in real time experiments. The simulation results are consistent with the experimental observations.

On the other hand, the trajectories in Figure 4A and Fig. S8 showed comparable growth rates in high expression state and in low expression state. It is possible that high expression cells in our study have not reached the threshold for significant metabolic burden to slow down the growth. The inhibition curves of the different inducer concentrations in Fig. 3B and the dynamic balance by intrinsic fluctuations also imply that the bimodality of the protein expression distribution is not due to cell growth.

Discussion

For self-repressor gene network, even when the gene is fixed, there can still be new cell phenotypes. Our study shows explicitly in this concrete gene circuit that different cell fates can emerge not only from the changes in the genes (such as mutations) but also from the changes in regulatory wirings or links through microenvironments without altering the gene itself. In fact, even when the topology of the wiring for the underlying gene regulatory network is fixed, there is still a possibility of cell phenotypic changes due to the changes in the regulation strengths induced by the environment. Furthermore, we observed both in real time experiments and simulations that the cell phenotypes or fates can be switched from one to the other. We also obtained the average time of this switching which quantifies how difficult it is

to communicate globally from one cell fate to the other. Therefore, using real time trajectories, we determine both the speed and the underlying processes of the cell fate decision-making/phenotypic state-switching.

Epigenetic effects are often challenging to study in eukaryotic cells. Our study in bacteria illustrates how the environments can influence the cell fates and cell fate decision-making in a controllable way. The experiments in bacteria are relatively easy and straightforward to perform and control. The epigenetic and micro-environmental effects can be mimicked through the modulation of inducers in our study. This is an advantage of our approach. We plan to apply our method to a variety of core regulatory motifs and modules in the gene networks to investigate how the environments or epigenetics influence the cell fates and the cell fate decision-making processes.

Acknowledgments

We thank H. Bujard and B.L.Wanner for providing pZE11 and CRIM vector systems respectively, as well as for providing detailed information on their origins and growth conditions. We would also like to thank X. S. Xie for providing *E. coli* SX4. This work was supported by the National Science Foundation (NSF) with grant number 0947767, the National Science Foundation of China (NSFC) with grant number 91430217 and the Ministry of Science and Technology (MOST) of China with grant number 2016YFA0203200.

Author contributions

Z.L. Jiang and L. Tian, X.N. Fang, Q. Z. Dong, and J. Wang contributed to the experimental design. Z.L. Jiang, L. Tian, X. N. Fang and Q. Z. Dong conducted the experiments. K. Zhang, Q. Liu, Z.L. Jiang and L. Tian, X. Fang, and J. Wang contributed to data interpretation. Z.L. Jiang, L. Tian, X.N. Fang, E. K. Wang and J. Wang contributed to writing and revising the manuscript.

References

- [1] Elowitz MB, Levine AJ, Siggia ED, & Swain PS (2002) Stochastic gene expression in a single cell. *Science* 297(5584):1183-1186.

- [2] Kaern M, Elston TC, Blake WJ, & Collins JJ (2005) Stochasticity in gene expression: From theories to phenotypes. *Nat Rev Genet* 6(6):451-464.
- [3] Becskei A, Kaufmann BB, & van Oudenaarden A (2005) Contributions of low molecule number and chromosomal positioning to stochastic gene expression. *Nat Genet* 37(9):937-944.
- [4] Swain PS, Elowitz MB, & Siggia ED (2002) Intrinsic and extrinsic contributions to stochasticity in gene expression. *P Natl Acad Sci USA* 99(20):12795-12800.
- [5] Raj A & van Oudenaarden A (2008) Nature, Nurture, or Chance: Stochastic Gene Expression and Its Consequences. *Cell* 135(2):216-226.
- [6] Qi H, Blanchard A, & Lu T (2013) Engineered genetic information processing circuits. *WIREs Syst Biol Med* 5(3): 273-287.
- [7] Graf T & Enver T (2009) Forcing cells to change lineages. *Nature* 462(7273):587-594.
- [8] Fu WX, Ergun A, Lu T, Hill JA, Haxhinasto S, Fassett MS, Gazit R, Adoro S, Glimcher L, Chan S, Kastner P, Rossi D, Collins JJ, Mathis D, & Benoist C (2012) A multiply redundant genetic switch 'locks in' the transcriptional signature of regulatory T cells. *Nat Immunol* 13(10):972-980.
- [9] Takahashi K & Yamanaka S (2006) Induction of pluripotent stem cells from mouse embryonic and adult fibroblast cultures by defined factors. *Cell* 126(4):663-676.
- [10] Yamanaka S & Blau HM (2010) Nuclear reprogramming to a pluripotent state by three approaches. *Nature* 465(7299):704-712.
- [11] Yamanaka S (2009) Elite and stochastic models for induced pluripotent stem cell generation. *Nature* 460(7251):49-52.
- [12] Wang J, Xu L, & Wang EK (2008) Potential landscape and flux framework of nonequilibrium networks: Robustness, dissipation, and coherence of biochemical oscillations. *P Natl Acad Sci USA* 105(34):12271-12276.

- [13] Wang J, Zhang K, Xu L, & Wang E (2011) Quantifying the Waddington landscape and biological paths for development and differentiation. *P Natl Acad Sci USA* 108(20):8257-8262.
- [14] Wang J (2015) Landscape and flux theory of non-equilibrium dynamical systems with application to biology. *Adv Phys* 64(1):1-137.
- [15] Sasai M & Wolynes PG (2003) Stochastic gene expression as a many-body problem. *P Natl Acad Sci USA* 100(5):2374-2379.
- [16] Balazsi G, van Oudenaarden A, & Collins JJ (2011) Cellular Decision Making and Biological Noise: From Microbes to Mammals. *Cell* 144(6):910-925.
- [17] Liao C, & Lu T (2013) A minimal transcriptional controlling network of regulatory T cell development. *J Phys Chem B* 117(42):12995-13004.
- [18] Nevozhay D, Adams R, Murphy K, Josic K, Balázsi G (2009) Negative autoregulation linearizes the dose response and suppresses the heterogeneity of gene expression. *P Natl Acad Sci USA* 106(13):5123-5128
- [19] Koga M, Matsuda M, Kawamura T, Sogo T, Shigeno A, Nishida E, & Ebisuya M (2014) Foxd1 is a mediator and indicator of the cell reprogramming process. *Nat Commun* 5:3197.
- [20] Buganim Y, Faddah DA, & Jaenisch R (2013) Mechanisms and models of somatic cell reprogramming. *Nat Rev Genet* 14(6):427-439.
- [21] Pijnappel WWMP, Esch D, Baltissen MPA, Wu GM, Mischerikow N, Bergsma AJ, van der Wal E, Han DW, vom Bruch H, Moritz S, Lijnzaad P, Altelaar AFM, Sameith K, Zaehres H, Heck AJR, Holstege FCP, Schöler HR, & Timmers HTM (2013) A central role for TFIID in the pluripotent transcription circuitry. *Nature* 495(7442):516-519.
- [22] Singh A & Weinberger LS (2009) Stochastic gene expression as a molecular switch for viral latency. *Curr Opin Microbiol* 12(4):460-466.
- [23] Yu J, Xiao J, Ren XJ, Lao KQ, & Xie XS (2006) Probing gene expression in live cells, one protein molecule at a time. *Science* 311(5767):1600-1603.

- [24] Thattai M & van Oudenaarden A (2001) Intrinsic noise in gene regulatory networks. *P Natl Acad Sci USA* 98(15):8614-8619.
- [25] Becskei A & Serrano L (2000) Engineering stability in gene networks by autoregulation. *Nature* 405(6786):590-593.
- [26] Lutz R & Bujard H (1997) Independent and tight regulation of transcriptional units in *Escherichia coli* via the LacR/O, the TetR/O and AraC/I-1-I-2 regulatory elements. *Nucleic Acids Res* 25(6):1203-1210.
- [27] Hasty J, McMillen D, & Collins JJ (2002) Engineered gene circuits. *Nature* 420(6912):224-230.
- [28] Austin DW, Allen MS, McCollum JM, Dar RD, Wilgus JR, Sayler GS, Samatova NF, Cox CD, & Simpson ML (2006) Gene network shaping of inherent noise spectra. *Nature* 439(7076):608-611.
- [29] Maithreye R, Sarkar RR, Parnaik VK, & Sinha S (2008) Delay-Induced Transient Increase and Heterogeneity in Gene Expression in Negatively Auto-Regulated Gene Circuits. *Plos One* 3(8):e2972.
- [30] Guet CC, Elowitz MB, Hsing WH, & Leibler S (2002) Combinatorial synthesis of genetic networks. *Science* 296(5572):1466-1470.
- [31] Kepler TB & Elston TC (2001) Stochasticity in transcriptional regulation: Origins, consequences, and mathematical representations. *Biophys J* 81(6):3116-3136.
- [32] Hornos JEM, Schultz D, Innocentini GCP, Wang J, Walczak AM, Onuchic JN, & Wolynes PG (2005) Self-regulating gene: an exact solution. *Physical review. E, Statistical, nonlinear, and soft matter physics* 72(5 Pt 1):051907.
- [33] Feng HD, Han B, & Wang J (2011) Adiabatic and Non-Adiabatic Non-Equilibrium Stochastic Dynamics of Single Regulating Genes. *J Phys Chem B* 115(5):1254-1261.
- [34] Fano U (1947) Ionization yield of radiations. II. The fluctuations of the number of ions. *Phys. Rev* 72(1):26-29.
- [35] Baum LE & Petrie T (1966) Statistical Inference for Probabilistic Functions Of Finite State Markov Chains. *Ann Math Stat* 37(6):1554-1563.

Figure Captions

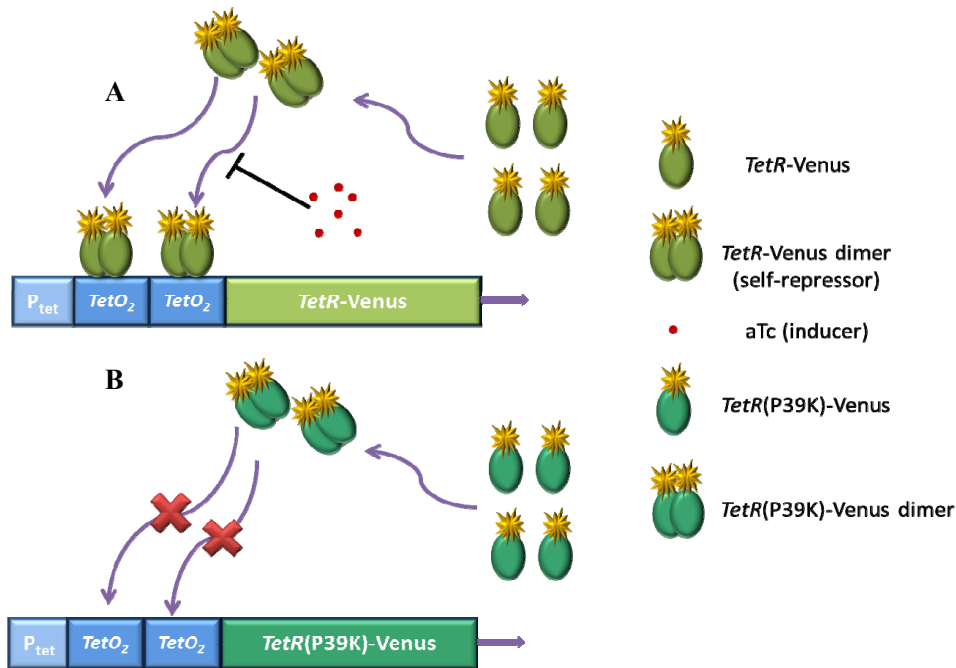


Figure 1: Schematic illustrations of the self-repressing gene circuit (MG::PR-8T) and the non-self-repressing gene circuit (MG::PR-8T-P39K). (A) Two *tet* operator sequences ($TetO_2$) inserted downstream of the P_{tet} promoter are bound by $TetR$ self-repressor dimers. In the absence of aTcs (the inducers), $TetR$ -Venus dimers bind to the operators. This interaction prevents the binding of RNA polymerase, thereby inhibiting the $TetR$ -Venus fusion protein synthesis. When aTcs diffuse into the cell, they bind to $TetR$, inducing an allosteric conformational change in the repressor protein which releases it from DNA, allowing for the possibility of the gene being switched into the “on” state. All of these constitute a self-repressing gene circuit. (B) The $TetR$ -P39K mutant is not capable of recognizing the operators and is unable to repress the $TetR$ -Venus expression, constituting a non-self-repression gene circuit.

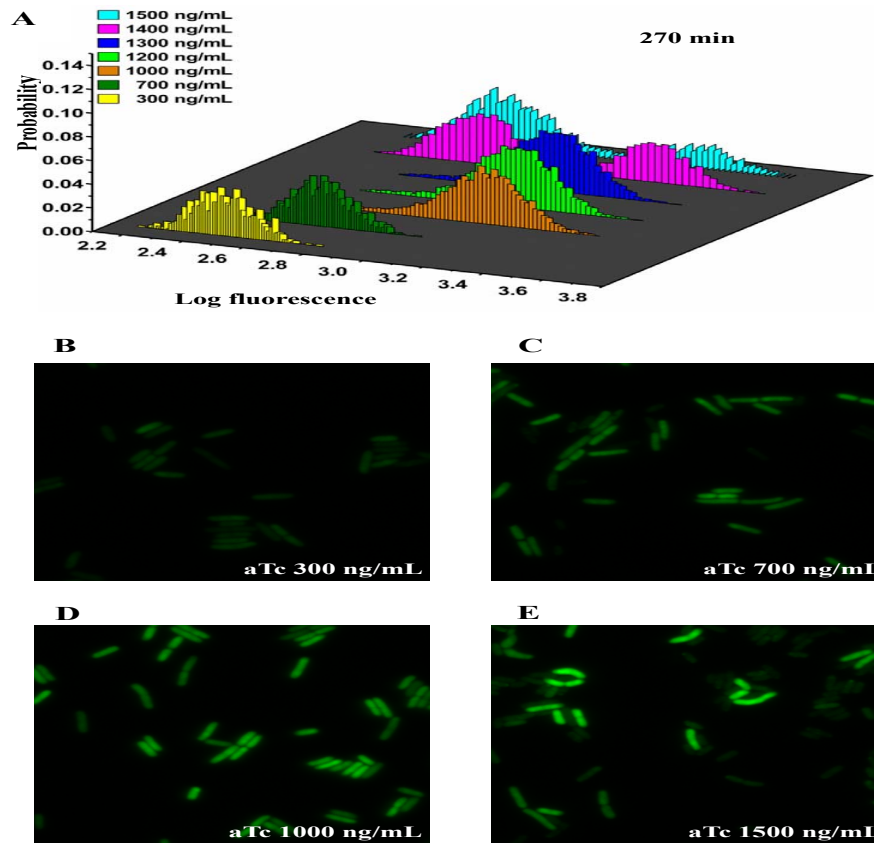


Figure 2: Experimental expression distributions of the self-repressing gene circuit (MG::PR-8T) at different aTc concentrations observed under a microscope. (A) In M9 media with the inducer concentrations ranging from 300 to 1500 ng/mL of aTcs, the resulting steady state fluorescence distributions show that the ratio of the populations of the bimodal fluorescence distributions depend on the aTc concentration. Seven color histograms represent different inducer concentrations. (B, C, D, and E) Four representative fluorescence images at different concentrations of aTcs (300, 700, 1000, and 1500 ng/mL) are selected.

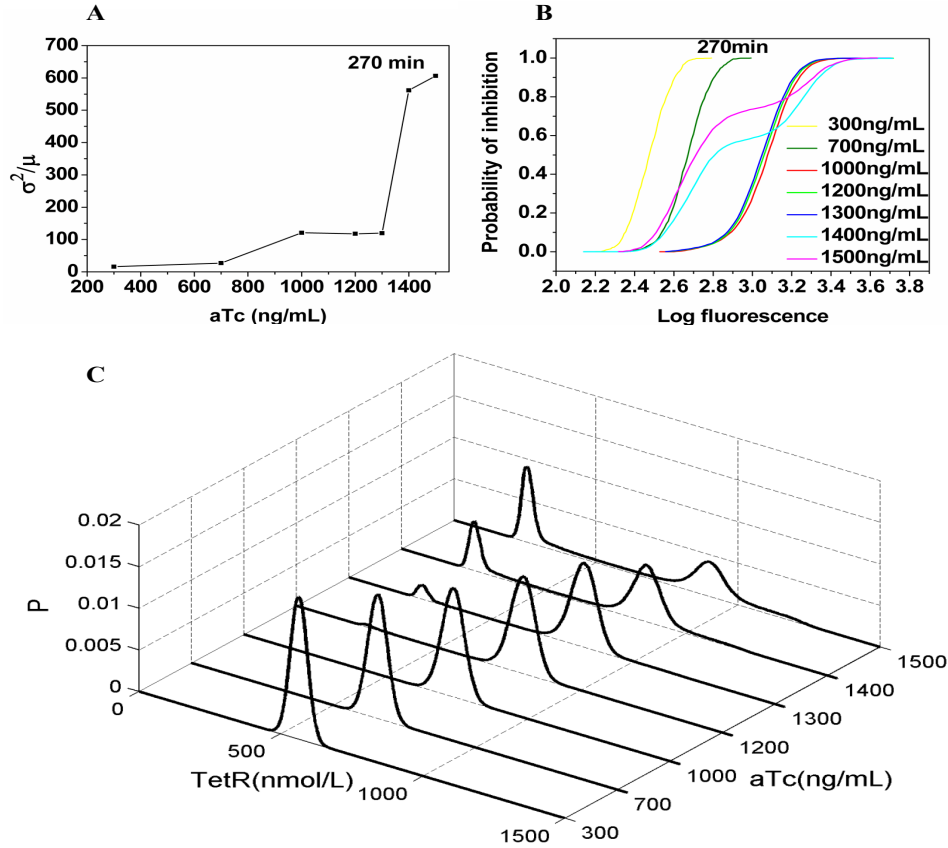


Figure 3: The Fano factor curves and the probability of inhibition curves of the self-repressing gene circuit. (A) Dose-response of the Fano factor ($F = \sigma^2/\mu$) of the *TetR*-Venus expression for the self-repressing gene circuit (MG::PR-8T) at different inducer concentrations. The Fano factor is defined as σ^2/μ , where σ^2 and μ are the variance and the mean of the probability distribution. (B) The probability of inhibition curves of the MG::PR-8T circuit at different inducer concentrations. Seven color histograms represent different inducer concentrations. The inhibition curves were obtained by the ratio of the cells with a fluorescence intensity lower than a certain value to the number of the total samples. (C) The probability distribution of the *TetR* proteins for the circuit of MG::PR-8T with different concentrations of inducers from the stochastic simulation model. $P(n)$ (z axis) represents the probability distribution of the TetR protein numbers (x axis), n at different numbers of inducer (aTc) molecules (y axis).

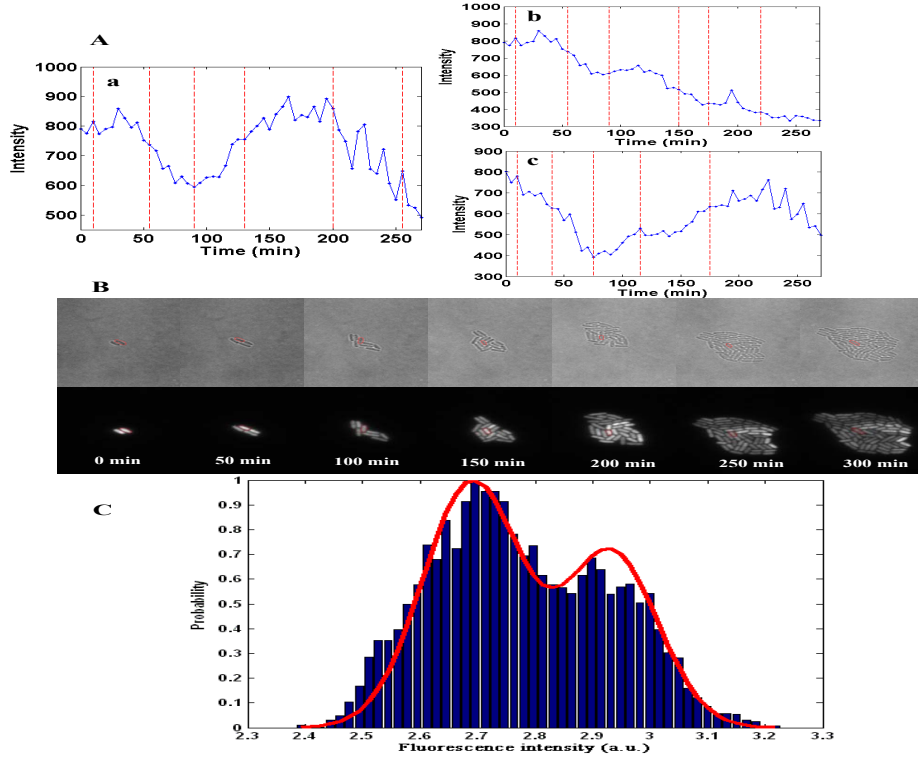


Figure 4: The mean fluorescence intensity distribution of the dynamical trajectories for MG::PR-8T Single cell mean fluorescence intensities were captured every 5 minutes. 28 micro-colonies were tracked by time-lapse microscopy. (A) Three representative single cell fluorescence trajectories induced by 1500 ng/mL aTcs. Points represent experimental fluorescence values. Red vertical dashed lines demarcate cell divisions. (B) The bright field and fluorescent field images of the corresponding measurements in the time-lapse experiment. The cells corresponding to the fluorescence trajectory in Fig. 4a are marked with red circles. The average of bacteria mean fluorescence intensity is 556 and the average cell cycle time is 46 minutes in this micro-colony. (C) The histogram gives the intensity distribution of the 163 single cell fluorescence trajectories induced at 1500 ng/mL aTc collected from the time-lapse experiments. The red solid curve is the fitted intensity distribution from HMM.